Int. J. Electrochem. Sci., 17 **(2022)** Article Number: 220443, doi: 10.20964/2022.04.44

International Journal of
ELECTROCHEMICAL
SCIENCE
www.electrochemsci.org

A Highly Sensitive Electrochemical Methamidophos Immobilized AChE Biosensor for Organophosphorus Pesticides Detection

Kai Zhang[1], *Liangzi Wang*[2], *Jingitao liu*[1], *Shiyu Zhao*[1], *Longfei Ding*[1], *Binhua Zhou*[1], *Bo Zhao*[1,*]

[1] National and Local Joint Engineering Research Center of Biomedical Functional Materials, School of Chemistry and Materials Science, Nanjing Normal University, Nanjing 210023, China
[2] Technical Center Animal Plant & Food Inspection and Quarantine, Shanghai Customs, Shanghai 200137, China
[*]E-mail: zhaobo@njnu.edu.cn

Received: 12 December 2021 / *Accepted:* 4 February 2022 / *Published:* 4 March 2022

Despite the harmful effects of organophosphorus pesticides (OPPs), few rapid detection methods of OPPs multi-residue have been practically applied; thus, it is important to improve existing methods and develop rapid detection methods and techniques. Reduced graphene oxide-chitosan (RGO-CHI)/methamidophos electrochemical biosensor was developed to detect multiple OPPs based on the principle of acetylcholinesterase (AChE) activity inhibition in the presence of OPPs. One OPP (methamidophos) that can combine with AChE in the incubation solution was immobilized on the electrode. The proposed method shows good linear relationships of nine OPPs and methomyl, a carbamate pesticide, with limits of detection between 0.05 and 0.52 ppb, indicating high accuracy for the application in real sample detection.

Keywords: Organophosphorus pesticides; highly sensitive electrochemical biosensor; AChE activity inhibition; multi-residue organophosphorus pesticides detection

1. INTRODUCTION

Organophosphorus pesticides (OPPs) are widely used in agricultural production [1,2], primarily for the prevention and control of plant diseases, insects, and grass damage [3]. OPPs have a strong effect on agricultural disease prevention; and the improvement of agricultural product yield [4,5]. However, OPPs are highly toxic to mammals as irreversible acetylcholinesterase (AChE) inhibitors [6]. The mechanism of organophosphate poisoning is that organophosphorus combines with AChE to form phosphorylated acetylcholinesterase, resulting in catalytic effect loss [7]. Also, the possible residues of OPPs in vegetables and fruits seriously affect human health and food safety, due to their widespread abuse and acute toxicity, which has attracted increasing public attention. With people's awareness of

agricultural product safety increasing, the continuous development of pesticide detection technology has been promoted. Although the conventional methods for OPPs detection using chromatography [8-10], capillary electrophoresis [11-13], and immunoassay [14-16]; have presented accurate results, these methods are complex and require skilled operators. Required measuring instruments are also expensive and inconvenient, and the identification specificity of OPPs is unsatisfactory. Due to the numerous samples required to be tested, most of these complex testing methods cannot meet the need for accurate and rapid detection methods.

Currently, many studies of the rapid detection of OPPs have been reported. However, some current detection methods cannot meet a high detection limit or the requirements of national standards. Many technologies are not credible, producing many false-positives and negatives. For some assays based on modified AChE, the maintenance of enzyme activity and the storage conditions of the sensors or kits should be considered. Also, some reported methods constructed based on the inhibition of AChE [17] or using aptamers [18] can only specifically detect one or several pesticides [19]. Montali et al [20] used a compact 3D-printed device for a CL foldable paper-based biosensor for the on-site detection of chlorpyrifos. The method has a linear relationship in the range of 0.01-10 mM with a limit of detection of 45.0 μM. Another noteworthy result is that Wu et al [21] proposed an approach for the synthesis of PDA-capped bimetallic AuPt hydrogels to immobilize AChE on the sensing interface and applied noble metal hydrogels to the electrochemical biosensor of OPPs detection for the first time. The biosensor has good stability, a wide linearity range, and high selectivity with the lowest detection limit of 0.185 ng/L. Regrettably, the reported assays have not addressed the instability of the detection results due to the maintenance of acetylcholinesterase activity. Hence, these methods are unsuitable for rapid and multi-residue detection of OPPs, which are limited to popularize and apply in practical detection [22]. Thus, existing methods must be improved to develop rapid multi-residue methods and techniques for OPPs detection in practical applications.

Fortunately, the application of nanomaterials could increase OPPs detection sensitivity [23]. Nanomaterials have many advantages in experimental research, such as the small size effect; surface and interface effects; quantum size effect; dielectric confinement effect; and macroscopic quantum tunneling effect [24-26], which could be thus considered as ideal bioreceptors, for constructing electrochemical biosensors. Graphene has been widely developed in many fields, particularly in sensor research, which is primarily due to its excellent properties, including its morphological structure, electrochemical properties [27], mechanical properties, selective properties with a large specific area, Raman spectral properties, and thermal properties [28]. Graphene has good adsorption performance and can be used as a carrier film for adsorbing molecules, which can interact with many substances to form a composite functional material with superior performance. ZrO_2NPs decorated graphene nanosheets hybrid was synthesized to fabricate a sensitive enzymeless methyl parathion sensor with a detection limit of 0.6 ng/mL by Gong et al [29].

Also, the modification of small molecules is relatively easy to achieve, and the small molecules can compensate for some problems that arise in the modification of AChE, such as harsh storage conditions and easy loss of enzyme activity, which can hinder the practical application of electrochemical biosensors. Cui et al. [30] immobilized AChE via adsorption onto chitosan, TiO_2, and reduced graphene oxide nanocomposites to construct an enzyme biosensor for OPPs detection. The

AChE biosensor showed good performance in detecting DDVP; however, the fabricated electrode must be kept at 4 °C to maintain enzyme activity.

We applied herein graphene and modified small molecules in the preparation process of the biosensor to develop a method that can be used in the rapid detection of OPPs, breaking the current bottleneck of OPPs detection. In this study, we constructed a multi-residue electrochemical biosensor based on AChE activity-inhibited by immobilizing the methamidophos that can bind to AChE with loss of enzyme activity. The sensitive changes of electrochemical signal caused by the combination of AChE and OPPs enabled us to quantify the OPPs in the fruit samples.

2. EXPERIMENTAL

2.1 Materials and Reagents.

Phoxim, dichlorvos, chlorpyrifos, and methamidophos were obtained from the official website of the National Standards Center. Parathion, pirimiphos-methyl, trichlorfon, dimethoate, omethoate, diazinon, fenthion, methomyl, chitosan, and graphene were purchased from Aladdin Biochemical Technology Co., Ltd. (Shanghai, China). Acetylcholinesterase (AChE) was obtained from Shanghai Enzyme-linked Biotechnology Co., Ltd. (Shanghai, China). Bovine serum albumin (BSA), potassium ferricyanide and phosphate-buffered saline (PBS, 10 mM, pH = 7.4) were ordered from Sinopharm Chemical Reagent Co., Ltd. (Shanghai, China), respectively. The water used in the experiment was secondary distilled water. Other reagents were analytical reagent grade.

2.2 Apparatus

A CHI660E electrochemical workstation (Shanghai Chenhua Instrument Co., Ltd., China) was used for electrochemical detection. A three-electrode system (Ag/AgCl (saturated KCl) electrode as the reference electrode, Pt wire electrode as the counter electrode, and glassy carbon electrode (GCE) as the working electrode) was used for electrochemical tests at room temperature. A UV1700PC ultraviolet spectrophotometer (Shanghai Phoenix Optical Instrument Co., Ltd, China) was used to characterize the combination of methamidophos and RGO-CHI.

2.3 Preparation of reduced graphene-chitosan complex (RGO-CHI)

Graphene oxide (GO) was prepared by the method proposed by Hummers [31]. Briefly, 0.625 mL of prepared GO suspension was gradually added to 100 mL of 0.1 M hydrochloric acid chitosan, and the solution was stirred at a constant temperature of 85 °C until brown. Then, 100 mg of ascorbic acid solid was added and stirred at a constant temperature of 60 °C. Finally, the solution was kept at room temperature. After being filtered, the prepared RGO-CHI was preserved at a low temperature.

2.4 Pretreatment of glassy carbon electrode

The glassy carbon electrode (GCE, diameter of 3 mm) was polished by 1.0 μm α-alumina power when the electrode surface was unclean or scratched. The electrode was polished by metallographic sandpaper (1200 W grits) until the scratch could be rid of. Then, the electrode was polished with 1.0, 0.3, and 0.05 μm γ-alumina powder. After sonicating in ethanol (*v:v*=1:1) and distilled water for 5 min in sequence, cyclic voltammetry (CV) was performed to test the value of ΔEp. Until ΔEp is below 70 mV, the electrode can be used for the following experiment. The electrode was rinsed thoroughly in distilled water and then dried in a vacuum for subsequent modification.

2.5 Preparation of RGO-CHI/methamidophos Electrochemical Biosensor

An RGO-CHI complex suspension with a volume of 10 μL was dripped onto the pre-treated electrode and kept at 37 °C until the surface dried. RGO-CHI was assembled on the surface of the GCE to obtain the modified electrode called RGO-CHI. Then, a 2.5-μL aliquot of methamidophos standard solution (0.2 g/L) was dripped onto the electrode surface for 30 min at 30 °C. Also, immersing the modified electrode in BSA solution (0.05%) for 30 min can make the active sites locked. Then, the active sites could not be combined with the methamidophos to eliminate the nonspecific adsorption of other substances on the electrode surface. After immersing the electrode in PBS solution (washing buffer), the multi-residue electrochemical biosensor called RGO-CHI/methamidophos was obtained.

2.6 Electrochemical characterization

Cyclic voltammetry (CV) was performed in a PBS buffer solution containing 2 mM of $K_3[Fe(CN)_6]$ to characterize every step of the electrochemical biosensor preparation process. The CV parameters were as follows: the scan range was -0.2 V to 0.8 V *vs.* Ag/AgCl; and the scan rate was 100 mV/s. Electrochemical impedance spectroscopy (EIS) was performed in a 0.1 M KCl solution containing 5 mM of $K_3[Fe(CN)_6]$ to characterize the sensitive change of the electrode surface. The EIS parameters were as follows: the low frequency was 0.01Hz, the high frequency was 10^6 Hz, and the amplitude was 5 mV. Differential pulse voltammetry (DPV) tests were performed in a PBS buffer solution containing 2 mM of $K_3[Fe(CN)_6]$ to characterize every step of the electrochemical biosensor preparation process. The DPV parameters were as follows: the potential range was -0.2 V to 0.5 V, and the pulse amplitude is 50 mV.

Similarly, the prepared RGO-CHI/methamidophos electrochemical biosensor for the detection of different concentrations of OPPs was characterized by DPV with the same parameters.

2.7 Computer simulation

The electrophorus electricus acetylcholinesterase crystal structure was downloaded from the RCSB PDB (https://www.rcsb.org/) with PDB ID 1C2O [32]. The 3D structures of OPPs (parathion, pirimiphos-methyl, trichlorfon, dimethoate, omethoate, diazinon, fenthion, phoxim, dichlorvos,

chlorpyrifos, methamidophos, and methomyl) were created and then prepared using the Lig Prep module of Maestro version 10.2 (Maestro 2015) software. Molecular docking was used to investigate the combination of OPPs or methomyl and AChE using the Glide module of Maestro 2015 program. The protein was processed by the Maestro 2015 program (Schrödinger software), including adding hydrogens, removing water molecules, and minimizing energy with the OPLS-3 force field. Then, the receptor grid was generated when centered on key amino acids (SER 203) with a 15 × 15 × 15 Å cube box. The ligands were docked into the AChE catalytically active site contained in the grid. The generated docked conformations were evaluated by Glide and the binding regions of OPPs with AChE were analysed.

3. RESULTS AND DISCUSSION

3.1 Characterization of RGO-CHI-methamidophos complex

A total of 20 times the amount used in the electrochemical biosensor preparation was used to verify the combination of methamidophos and RGO-CHI into a composite. The UV-Vis absorption spectra [33] of the RGO-CHI-methamidophos complex, RGO-CHI complex and methamidophos were measured with distilled water as the reference. The parameters were as follows: the wavelength scanning range was 190-800 nm, and the scanning interval was 0.5 nm. As shown in Figure 1, the characteristic absorption peaks of methamidophos solution and RGO-CHI are 210 nm and 262 nm, while a new characteristic peak at 265 nm is the characteristic peak of the RGO-CHI-methamidophos complex, which indicates the combination of methamidophos and RGO-CHI.

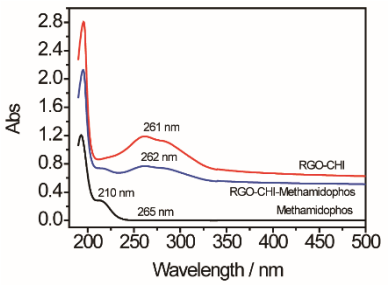

Figure 1. UV-Vis absorption spectra of the RGO-CHI-methamidophos complex.

3.2 Computer simulation analysis

The aromatic organophosphorus pesticide parathion, as recognition molecule, is useful for organophosphorus pesticides detection based on enzyme inhibition activity [34]. In this study, the OPPs and methomyl were docked into the active sites of the AChE enzyme. Docking process was carried out by Glide module (Maestro 2015 program) to investigate the intermolecular forces of OPPs or methomyl and AChE. Glide performs a comprehensive and systematic search of the conformation, orientation, and positional space of docked ligands, and also searches for potential positions of these ligands in the receptor's active site [35]. The docking results of pesticides are shown in Table 1. Simultaneously, results

suggest that parathion would bind AChE with the strongest intermolecular forces. Furthermore, from the molecular simulation perspective, the modification of parathion is more likely to be successful than other molecules when applied to the electrode surface. The docking scores in the range of -4.078 to -5.727 kcal/mol of OPPs and the various intermolecular forces indicated that different OPPs do not have the same effect on AChE activity. To investigate the feasibility of fatty molecules modified on the electrodes, we analysed the intermolecular forces of AChE and pesticides. Figure 2 shows the interaction of AChE and methamidophos, which binds best to acetylcholinesterase. Two hydrogen bonds exist between the two H atoms in the amino group of methamidophos and the double-bonded oxygen atom of the carboxyl groups of GLY 120 (1.9 Å) and GLH 202 (2.0 Å), respectively. Hydrophobic interactions are present between methamidophos and some amino acids of AChE (TRP 86, TRP 117, TYR 119, and PRO 446). This result is consistent with the experimental results that both organophosphorus and carbamate pesticides can inhibit AChE activity [36]. Simulations show that methamidophos can be used as a recognition molecule immobilized on the electrode surface to construct a new electrochemical biosensor for OPPs detection.

Table 1. Docking results of all pesticides.

Pesticides	Docking score (kcal / mol)	Glide energy (kcal / mol)	Glide einternal (kcal / mol)	Glide emodel (kcal / mol)
parathion	-5.727	-29.671	9.698	-38.007
diazinon	-5.698	-35.806	8.358	-43.066
phoxim	-5.687	-34.622	2.126	-44.450
pirimiphos-methyl	-5.359	-27.299	7.816	-32.570
methamidophos	-5.258	-22.925	1.745	-29.231
omethoate	-5.210	-33.887	4.454	-42.127
fenthion	-5.169	-25.938	0.658	-33.668
chlorpyrifos	-4.904	-35.267	6.785	-39.658
dichlorvos	-4.870	-28.709	0.443	-37.100
dimethoate	-4.800	-30.191	7.191	-36.391
trichlorfon	-4.453	-27.308	6.675	-31.958
methomyl	-4.078	-28.048	9.969	-30.241

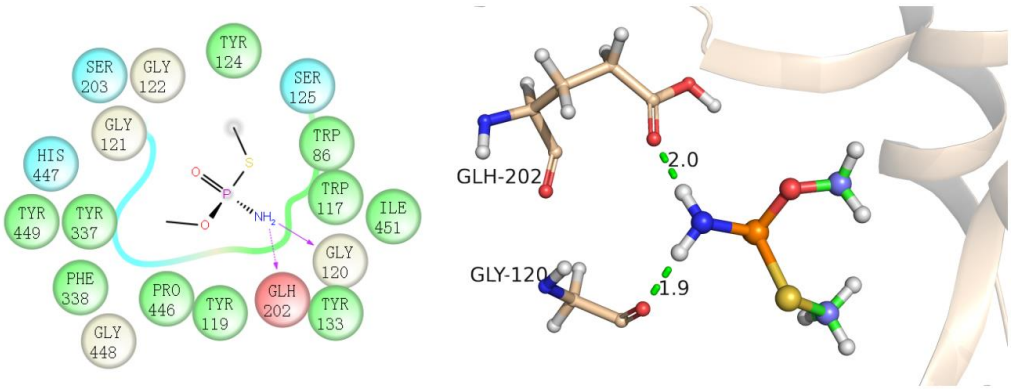

Figure 2. Docking result of AChE with OPP (OPP in the figure is methamidophos).

3.3 Principle of RGO-CHI/methamidophos Electrochemical Biosensor

As shown in Scheme 1, the detection principle of the RGO-CHI/methamidophos electrochemical biosensor for sensitive detection of multiple OPPs is depicted. The modified RGO-CHI/methamidophos electrode was applied to detect a series of standard solutions of OPPs containing AChE.

The AChE in the incubation solution completely reacted with methamidophos to form phosphorylated acetylcholinesterase in the absence of OPPs, which then hindered electron transfer [37]. DPV was characterized by significant changes in the current value. The detection of organophosphorus pesticides by the change of DPV peak current value has been successfully applied [1, 37, 38]. The OPPs in the incubation solution and the methamidophos on the electrode surface competitively combine with AChE in the incubation solution. Both the methamidophos modified on the electrode surface and the OPPs in the incubation solution could inhibit the AChE activity, while the AChE bound with the methamidophos modified on the electrode surface could generate decreased current signals. The more OPPs in the incubation solution, the fewer methamidophos on the electrode surface bind to AChE, resulting in a smaller peak current value. The inverse proportionality of the reduced peak current to the concentration of OPPs lays the foundation for organophosphorus pesticide detection. Accordingly, a good linear relationship can be established between the change amount of peak current (where $\Delta I = I_x - I_0$, I_x is the DPV peak current obtained by measuring OPPs with different concentrations, and I_0 is the DPV peak current obtained by measuring the blank sample) and the concentration of the OPPs standard solution.

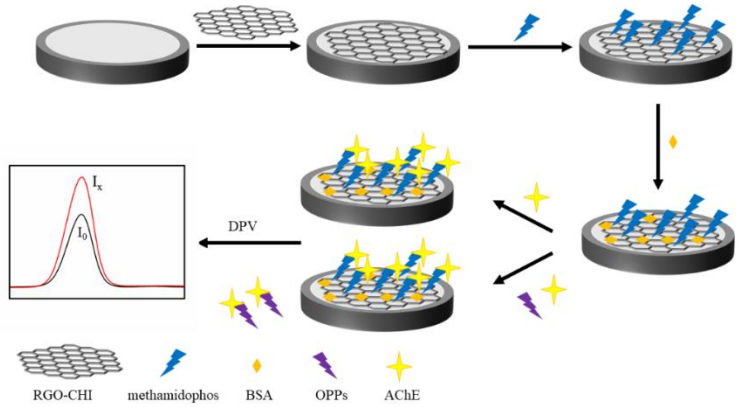

Scheme 1. Schematic illustration of the RGO-CHI/methamidophos electrochemical biosensor for OPPs detection.

3.4 Feasibility of the RGO-CHI/methamidophos electrochemical biosensor

To verify the feasibility of this method, we performed CV tests and EIS tests to characterize different steps of the preparation process of the electrochemical biosensor. The response of CV tests is shown in Figure 3A, indicating that the bare GCE shows stable redox characteristic peaks of $K_3[Fe(CN)_6]/K_3[Fe(CN)_6]$ with ΔEp values below 70 mV (Curve a, Figure 3A). When the RGO-CHI complex was modified on the GCE, electron transfer was accelerated [39], resulting in an increased CV current value (Curve b, Figure 3A), which can be attributed to the outstanding electrical conductivity of RGO [40]. However, after methamidophos was modified, electron transfer on the electrode surface was

blocked, resulting in a decreased CV current (Curve c, Figure 3A). With AChE in the incubation solution, the current decreases further, ascribing to the formation of phosphorylated acetylcholinesterase [41] causing higher hindrance of electron transfer (Curve d, Figure 3A). Therefore, the sensitive current change caused by the inhibited enzymatic activity of AChE coupled with the accumulation of phosphorylated acetylcholinesterase is regarded as a feasible tool for OPPs detection.

EIS tests were performed to characterize the sensitive change of the electrode surface [42]. Figure 3B shows the electrochemical impedance spectroscopy of different steps of the preparation process. The R_{et} of the bare GCE was approximately 80 Ω (Curve a, Figure 3B). A decreased R_{et} of approximately 50 Ω (Curve b, Figure 3B) was obtained, due to the modification of RGO-CHI which can markedly enhance the conductivity on the GCE surface. After the modification of methamidophos on the above GCE surface, electron transfer was blocked, resulting in an increased R_{et} of approximately 110 Ω (Curve c, Figure 3B). However, R_{et} continued to increase to 130 Ω (Curve d, Figure 3B), after the active site surface was sealed with BSA. Finally, when the biosensor was immersed in the AChE solution with OPPs, R_{et} increased to 150 Ω, indicating that methamidophos on the electrode surface combined with AChE (Curve e, Figure 3B). However, without OPPs in the AChE solution, R_{et} decreased further to 200 Ω, ascribing to the formation of phosphorylated acetylcholinesterase causing higher hindrance of electron transfer (Curve f, Figure 3B). Thus, the biosensor was successfully prepared and feasible for application in OPPs detection according to the electrochemical characterization results.

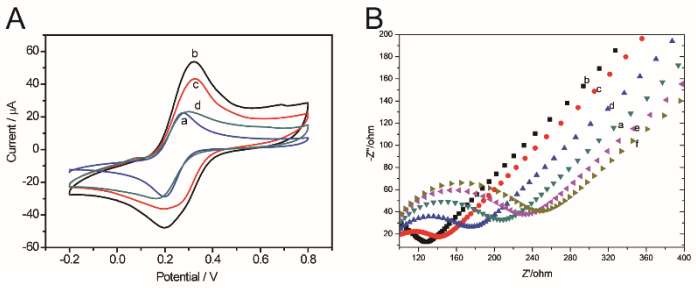

Figure 3. (A) CV response of the RGO-CHI/methamidophos electrochemical biosensor at different stages: (a) bare GCE; (b) RGO-CHI; (c) RGO-CHI/methamidophos; (d) RGO-CHI/methamidophos/AChE. (B) EIS response of RGO-CHI/methamidophos electrochemical biosensor at different stages: (a) bare GCE; (b) RGO-CHI; (c) RGO-CHI/methamidophos; (d) RGO-CHI/methamidophos/BSA; (e) RGO-CHI/methamidophos/AChE with OPPs; (f) without OPPs.

3.5 Optimization of Experimental Conditions

A series of factors including the AChE concentration and the AChE incubation time were investigated in this study to explore the best experimental conditions of the biosensor. Because the detection of OPPs is based on the combination of AChE and OPPs in this study, the concentration of AChE must be investigated. The effect of the concentration of AChE was optimized and the results were determined by DPV. The electrode was incubated in AChE solutions of different concentrations. As shown in Figure 4A, as the AChE concentration increased, the peak current decreased continuously. When the AChE concentration reached 8 $U \cdot mL^{-1}$, as the concentration of AChE increased, the peak

current value changed negligibly, indicating that the amount of AChE modified on the electrode surface reached the maximum [43]. Therefore, 8 $U \cdot mL^{-1}$ was chosen as the optimal AChE concentration for subsequent experiments.

Then, the influence of the incubation time of AChE was investigated. Figure 4B shows that the peak current of the electrochemical biosensor decreased gradually over the incubation time range of 5-30 min, and the peak current tended to remain unchanged as the binding time reached 25 min, showing that the binding of methamidophos and AChE was saturated. Thus, 25 min can be taken as the optimal incubation time of AChE.

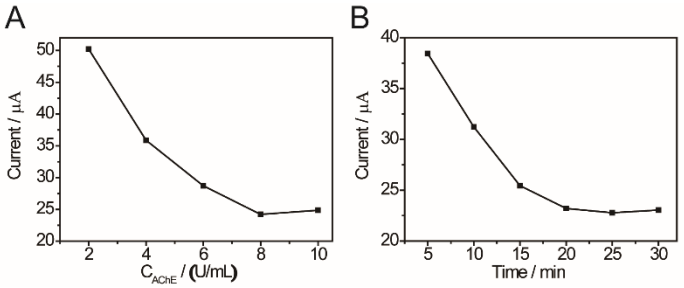

Figure 4. Optimization of (A) concentrations of AChE, (B) incubation time of AChE.

3.6 Detection of OPPs

Under optimal experimental conditions, an RGO-CHI/methamidophos electrochemical biosensor could detect OPPs (e.g., dichlorvos, chlorpyrifos, methamidophos, parathion, pyrimidin methyl, trichlorfon, dimethoate, omethoate, diazinon, fenthion) and carbamate pesticides (e.g., methomyl). The DPV response was used to characterize different concentrations of OPPs standard solutions. AChE activity inhibition in the presence of OPPs resulted in a change in the electrochemical signal. The multi-residue biosensor could be constructed utilizing AChE as a recognition substrate of various OPPs. The detection curves detected by DPV are shown in Figure 5. The more OPPs or methomyl in the incubation solution, the greater the difference in the DPV peak value, suggesting that the change in the DPV peak current is proportional to the concentration of OPPs and methomyl. The corresponding linear relationships between the change in peak current and the logarithm of OPPs and methomyl concentration, where linear regression equations can be established and the primary parameters of the electrochemical biosensor for detecting different targets, are shown in Table 2.

Presumably, the negligible difference in the slope value for OPPs (RSD value of 7.8%) could likely be explained by the formation of phosphorylated AChE; however, the difference in the slope of methomyl is much larger due to the formation of carbamyl AChE when methomyl combines with AChE. The different structures of phosphorylated AChE and carbamyl AChE may be related to the hindrance of electron transfer on the GCE surface.

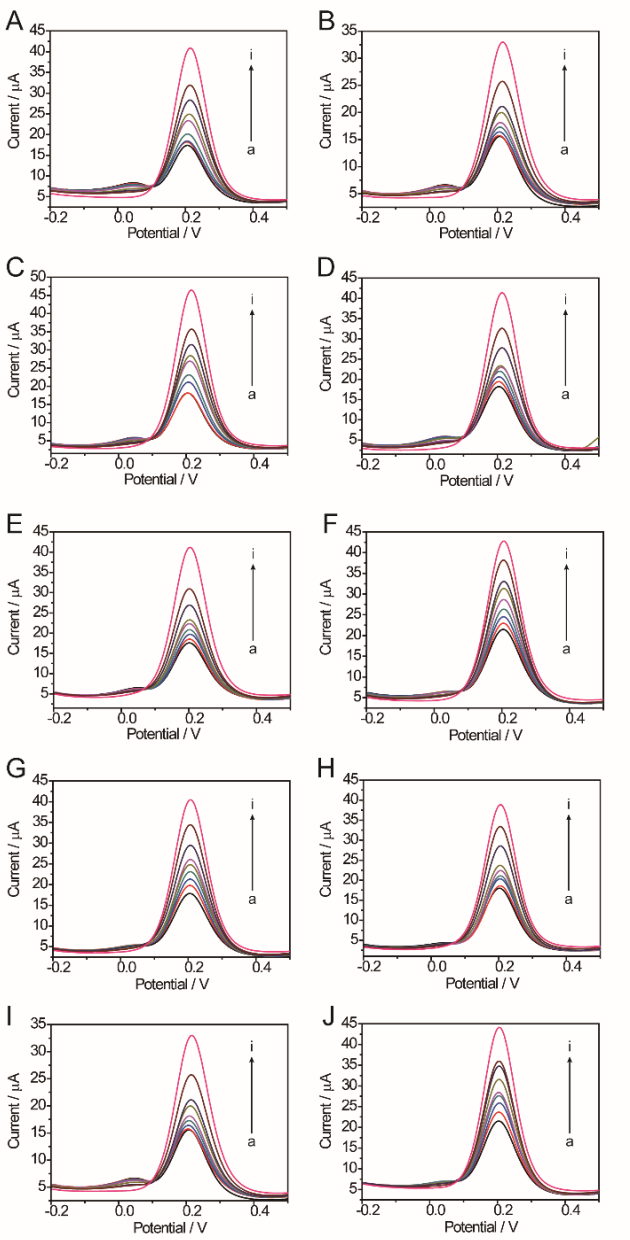

Figure 5. DPV response of different concentrations of (A) parathion, (B) dichlorvos, (C) chlorpyrifos, (D) methamidophos, (E) trichlorfon, (F) dimethoate, (G) omethoate, (H) diazinon, (I) fenthion, and (J) methomyl; the concentrations from a to i were 0, 1, 10, 100, 200, 400, 800, 1200, and 1500 ng/mL, respectively.

Additionally, we also compared the electrochemical method with some other detection methods. As shown in Table 3, this proposed assay can detect more pesticides than other methods and exhibits a linear range. The proposed assay based on AChE enzyme activity inhibition utilized methamidophos, binding to AChE with an irreversible reaction with loss of enzyme activity to achieve pesticides detection. The difference in detection sensitivity of various OPPs may be related to the different inhibition abilities to AChE. And the modification of methamidophos is relatively easy to achieve. These experimental results indicate that the electrochemical method could be a suitable method for OPPs detection.

Table 2. Primary parameters of the RGO-CHI/methamidophos electrochemical biosensor for detecting different targets (S/N=3)

Analyte	Linear range (ng/mL)	Linear equation	Correlation Coefficient (R)	Limit of detection (ng/mL)
Parathion	0-1500	ΔI=10.20+0.0154lgC	0.9927	0.21
Dichlorvos		ΔI=17.40+0.0156lgC	0.9953	0.06
Chlorpyrifos		ΔI=11.25+0.0158lgC	0.9929	0.39
Methamidophos		ΔI=17.90+0.0152lgC	0.9923	0.26
Trichlorfon		ΔI=14.92+0.0159lgC	0.9949	0.05
Dimethoate		ΔI=15.60+0.0153lgC	0.9920	0.16
Omethoate		ΔI=12.35+0.0167lgC	0.9966	0.09
Diazinon		ΔI=10.20+0.0154lgC	0.9927	0.52
Fenthion		ΔI=16.54+0.0162lgC	0.9931	0.25
Methomyl		ΔI=9.30+0.0106lgC	0.9966	0.05

Table 3. Comparison of different methods for OPPs detection.

Method	OPPs	Linear range ng/mL	Limit of detection ng/mL	Ref.
immunochromatographic assay	parathion	0.7−13.0	0.411	[16]
colorimetric assay using AuNPs as a probe	paraoxon, parathion, fenitrothion and diazinon	0.3–17.30	0.13–0.42	[17]
multilayer paper chip detection method	dipterex	50-500	40.6	[20]
dissociable photoelectrochemical sensor	paraoxon	0.05–10	0.017	[44]
RGO-CHI/methamidophos electrochemical biosensor	parathion, dichlorvos, chlorpyrifos, methamidophos, trichlorfon, dimethoate, omethoate, diazinon, fenthion, methomyl	0–1500	0.05–0.52	this work

3.7 Performance Test of RGO-CHI/methamidophos Electrochemical Biosensor

To demonstrate the reliable application of the proposed method, the following series of experiments were performed. The prepared biosensor was used to detect methamidophos of different concentrations using seven different electrodes, and the relative standard deviation (RSD) calculated was 4.3% to 9.5%. The result shows that the repeatability of the biosensor is acceptable [45].

Subsequently, to investigate the stability of the biosensor, it was stored at 37.4 ℃ for 1 day to 10 days. The peak current of methamidophos was then detected. The RSD of the slope of the standard curve obtained calculated by ten independent experiments was 5.7%. Thus, the proposed biosensor has good stability.

3.8 Detection in real samples

The concentrations of chlorpyrifos and dichlorvos in apple samples were measured using the standard addition method [46]. The pretreatment of real samples took the approach proposed in our previous study [34]. The recovery rate was determined, as shown in Table 3, to be between 85.19% and 137.03%, and the relative standard deviation was below 10%, which is acceptable, indicating that the RGO-CHI/methamidophos electrochemical biosensor can be used for OPPs detection.

Table 3. OPPs Detection in apple samples.

OPPs	Theoretical concentration (Experimental addition) (ng/mL)	Actual measured concentration (ng/mL)	Recovery rate （%）	Average recovery rate （%）	RSD（% ）
chlorpyrifos	100	85.19	85.19	90.70	6.36
		90.43	90.43		
		96.72	96.72		
	400	470.51	117.62	111.20	9.53
		392.52	98.13		
		472.21	118.05		
	900	1009.80	112.20	108.81	7.82
		1037.35	115.26		
		890.95	98.99		
dichlorvos	100	95.01	95.01	95.02	9.65
		85.84	85.84		
		104.19	104.19		
	400	473.58	118.39	119.43	3.24
		494.96	123.74		
		464.77	116.19		
	900	969.18	107.69	110.55	12.84
		1233.33	137.03		
		781.13	86.79		

4. CONCLUSION

An AChE biosensor based on the combination of AChE and OPPs and the excellent electrical conductivity of RGO for the detection of multiple OPPs was developed. The methamidophos was immobilized on the electrode. Compared with other assays, the proposed method can improve the broad spectrum of OPPs detection. The method also has versatility for various OPPs in real samples such as apples. The detection limits for different OPPs are between 0.05 ppb and 0.52 ppb. The biosensor prepared in this study exhibited good repeatability and stability. Moreover, the average recovery of standard addition in real sample detection was between 90.70% and 119.4%, demonstrating high accuracy for the developed assay in practical detection.

ACKNOWLEDGMENT
This work was supported by the National Key Research and Development Program of China (2020YFF0218301), and the Transformation of Scientific and Technological Achievements Programs of Higher Education Institutions in Shanxi (2020CG032).

References

1. Y. F. Zhao, R. S. Zheng, *Int. J. Electrochem. Sci*., 16 (2021) Article Number: 211221.
2. Y. H. Chu, Y. Li, Y. T. Wang, B. Li, and Y. H. Zhang, *Food Chem.*, 254 (2018) 80.
3. M. Majdinasab, M. Daneshi, and J. L. Marty, *Talanta*, 232 (2021) 122397.
4. C. S. Pundir, A. Malik, Preety, *Biosens. Bioelectron.*, 140 (2019) 111348.
5. Y. Hirata, K. Kuwabara, M. Takashima, and T. Murai, *Chem. Res. Toxicol.*, 33 (2020) 2892.
6. C. N. Pope, *J. Toxicol. Environ. Health, Part B*, 2 (1999) 161.
7. P. Norouzi, M. Pirali-Hamedain, M. Ganjali and F. Faridbod, *Int. J. Electrochem. Sci.*, 5 (2010) 1434.
8. X. J. Mao, W. M. Xiao, Y. Q. Wan, Z. M. Li, and D. M. Luo, *Food Chem.*, 345 (2021) 128807.
9. M. Tazarv, H. Faraji, A. Moghimi, and F. Azizinejad, *J. Sep. Sci*, 44 (2021) 2965.
10. I. Boneva, S. Yaneva, and D. Danalev, *Acta Chromatogr.*, 33 (2021) 188.
11. J. Li, J. X. Lu, X. G. Qiao, and Z. X. Xu, *Food Chem.*, 221 (2017) 1285.
12. D. Q. Li, X. G. Qiao, J. X. Lu, and Z. X. Xu, *Adv. Polym. Technol.*, 37 (2018) 968.
13. V.G. Amelin, D. S. Bol'shakov, and A. V. Tretyakov, *J. Anal. Chem.*, 67 (2012) 904.
14. M. D. Jiang, S. Wu, L. H. Xu, X. G. Qiao, and Z. X. Xu, *Food Agric. Immunol.*, 28(2017) 1242.
15. H. L. Wu, B. Z. Wang, Y. Wang, Z. L. Xiao, L. Luo, Z. J. Chen, Y. D. Shen, and Z. L. Xu, *Anal. Methods*, 13 (2021) 1911.
16. B. B. Liu, P. Li, Y. L. Wang, Y. R. Guo, H. X. Y. Zhang, S. Dong, Y. H. Xiong, and C. Z. Zhang, *Food Anal. Methods*, 13 (2020) 1736.
17. M. L. Satnami, J. Korram, R. Nagwanshi, S. K. Vaishanav, I. Karbhal, H. K. Dewangan, and K. K. Ghosh, *Sensors Actuat. B: Chem.*, 267 (2018) 155.
18. J. Y. Fu, X. S. An, Y. Yao, Y. M. Guo, and X. Sun, *Sensors Actuat. B: Chem.*, 287 (2019) 503.
19. M. Bhattu, M. Verma, and D. Kathuria, *Anal. Methods*, 13 (2021) 4390.
20. L. Montali, M. M. Calabretta, A. Lopreside, M. D'Elia, M. Guardigli, and E. Michelini, *Biosens. Bioelectron.*, 162 (2020) 112232.
21. Y. Wu, L. Jiao, W. Q. Xu, W. L. Gu, C. Z. Zhu, D Du, and Y. H. Lin, *Small*, 15 (2019) e1900632.
22. N. Yang, P. Wang, C. Y. Xue, J. Sun, H. P. Mao, and P. K. Oppong, *J.Food Process Eng.*, 41 (2018) e12867.

23. V. Kumar, K. Vaid, S. A. Bansal, and K. H. Kim, *Biosens. Bioelectron.*, 165 (2020) 112382.
24. H. Alam, S. Ramakrishna, *Nano Energy*, 2 (2013) 190.
25. S. A. Ansari, Q. Husain, *Biotechnol. Adv.*, 30 (2012) 512.
26. K. Ariga, H. Ito, J. P. Hill, and H. Tsukube, *Chem. Soc. Rev.*, 41 (2012) 5800.
27. S. C. Xu, Y. Y. Zhang, K. Dong, J. N. Wen, C. M. Zheng, and S. H. Zhao, *Int. J. Electrochem. Sci.*, 12 (2017) 3343.
28. Y. W. Zhu, S. Murali, W. W. Cai, X. S. Li, J. W. Suk, J. R. Potts, and R. S. Ruoff, *Adv. Mater.*, 22 (2010) 3906.
29. J. M. Gong, X. J. Miao, H. F. Wan, and D. D. Song, *Sensors Actuat. B: Chem.*, 162 (2012) 341.
30. H. F. Cui, W. W. Wu, M. M. Li, X. J. Song, Y. X. Lv, and T. T. Zhang, *Biosens. Bioelectron.*, 99 (2018) 223.
31. M. Wojnicki, M. Luty-Błocho, I. Dobosz, J. Grzonka, K. Pacławski, K. J. Kurzydłowski, and K. Fitzner, *Mater. Sci. Appl.*, 04 (2013) 162.
32. Y. Bourne, J. Grassi, P. E. Bougis, and P. Marchot, *J. Biol. Chem.*, 274 (1999) 30370.
33. N. I. Ikhsan, P. Rameshkumar, and N. M. Huang, *Electrochim. Acta*, 192 (2016) 392.
34. X. M. Xie, B. H. Zhou, Y. L. Zhang, G. Z. Zhao, and B. Zhao, *Chem. Phys. Lett.*, 767 (2021) 138355.
35. L. Gao, M. A. Zu, S. Wu, A. L. Lin, and G. H. Du, *Bioorg. Med. Chem. Lett.*, 21 (2011) 5964.
36. H. Schulze, S. V. F. Villatte, T. T. Bachmann, and R. D. Schmid, *Biosens. Bioelectron.*, 18 (2003) 201.
37. S. Li, L. M. Qu, J. F. Wang, X. Q. Ran, and X. Niu, *Int. J. Electrochem. Sci.*,15 (2020) 505.
38. M. Musameh, M.R. Notivoli, M. Hickey, C. P. Huynh, S. C. Hawkins, J. M. Yousef, and I. L. Kyratzis, *Electrochim. Acta*, 101 (2013) 209.
39. B. Wang, Y. Li, H. Y. Hu, W. H. Shu, L. Q. Yang, and J. H. Zhang, *PLoS ONE*, 15 (2020) e0231981.
40. S. J. Xu, L. Yong, and P. Y. Wu, *ACS Appl. Mater. Interfaces*, 5 (2013) 654.
41. K. A. LORD, C. POTTER, *Nature*, 166 (1950) 893.
42. G. Zhao, G. Li, X. C. Wang, G. Liu, and N. T. D. Thuy, *Int. J. Electrochem. Sci.*, 16 (2021) 150956.
43. G. Z. Zhao, B. H. Zhou, X. W. Wang, J. Shen, and B. Zhao, *Food Chem.*, 354 (2021) 129511.
44. Y. Qin, Y. Wu, G. J. Chen, L. Jiao, L. Y. Hu, W. L. Gu, and C. Z. Zhu, *Anal. Chim. Acta*, 1130 (2020) 100
45. C. C. Chang, C. H. Lai, C. H. Wang, Y. Liu, M. Shao, Y. H. Zhang, and J. L. Wang, *Atoms. Environ.*, 422 (2008) 6973.
46. L. Rubio, L. A. Sarabia, and M. C. Ortiz, *Talanta*, 138 (2015) 86.